

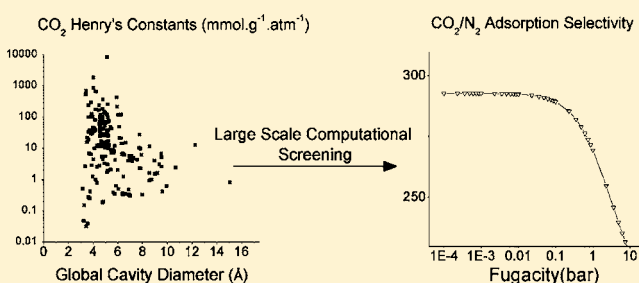
# Finding MOFs for Highly Selective CO<sub>2</sub>/N<sub>2</sub> Adsorption Using Materials Screening Based on Efficient Assignment of Atomic Point Charges

Emmanuel Haldoupis, Sankar Nair, and David S. Sholl\*

School of Chemical & Biomolecular Engineering, Georgia Institute of Technology, 311 Ferst Drive, Atlanta, Georgia 30332-0100, United States

**S** Supporting Information

**ABSTRACT:** Electrostatic interactions are a critical factor in the adsorption of quadrupolar species such as CO<sub>2</sub> and N<sub>2</sub> in metal–organic frameworks (MOFs) and other nanoporous materials. We show how a version of the semiempirical charge equilibration method suitable for periodic materials can be used to efficiently assign charges and allow molecular simulations for a large number of MOFs. This approach is illustrated by simulating CO<sub>2</sub> and N<sub>2</sub> adsorption in ~500 MOFs; this is the largest set of structures for which this information has been reported to date. For materials predicted by our calculations to have promising adsorption selectivities, we performed more detailed calculations in which accurate quantum chemistry methods were used to assign atomic point charges, and molecular simulations were used to assess molecular diffusivities and binary adsorption isotherms. Our results identify two MOFs, experimentally known to be stable upon solvent removal, that are predicted to show no diffusion limitations for adsorbed molecules and extremely high CO<sub>2</sub>/N<sub>2</sub> adsorption selectivities for CO<sub>2</sub> adsorption from dry air and from gas mixtures typical of dry flue gas.



## INTRODUCTION

The development of metal–organic frameworks (MOFs) and related crystalline nanoporous materials has led to intense interest in the use of these materials for chemical separations and other applications.<sup>1–5</sup> Computational modeling has become an important complement to experimental studies of MOFs.<sup>6,7</sup> Although much of the literature applying computational methods to MOFs has focused on detailed studies of individual materials, recent efforts have been made to expand the scope of these approaches to efficiently describe large numbers of materials. For example, we have recently introduced methods for this purpose that predict adsorption and diffusion properties of spherical nonpolar adsorbates in nanocrystalline materials and used these methods to study ~500 MOFs<sup>8</sup> and a collection of >250 000 hypothetical silica zeolites.<sup>9</sup> Recently another large scale computational approach was published by Wilmer et al.<sup>10</sup> describing the generation and computational screening of a library of >137 000 hypothetical MOFs for methane-storage applications.

To simulate the adsorption of quadrupolar or polar molecules inside MOFs, the electrostatic interactions between adsorbates and the MOF framework must be described. This is almost always accomplished by assigning point charges to each atom in the MOF and then summing the Coulomb interactions between atoms in adsorbing molecules and the MOF. The task of assigning point charges to MOFs has been examined extensively in recent years.<sup>6</sup> Most initial work on this topic used quantum chemistry calculations of finite clusters chosen to

represent the MOF of interest. The need to terminate clusters and choose cluster boundaries appropriately must always be addressed when using this approach. Methods suitable for assigning charges from density functional theory (DFT) calculations with the full periodic structure of MOFs have been developed that avoid this issue.<sup>11,12</sup> Very recently, Watanabe et al. showed that it is not necessary to assign point charges to MOF atoms to describe adsorption electrostatics in calculations where the MOF is assumed to be rigid.<sup>13</sup> In this case, one can directly use the electrostatic potential energy surface (EPES) computed from a periodic DFT calculation to define the electrostatic properties of adsorbed molecules.

The methods for describing electrostatics during adsorption in MOFs reviewed above are well suited to examining individual materials of interest, but are not as well suited for efficiently examining large numbers (hundreds or thousands) of materials. To accomplish this goal, there is considerable value in using methods that have low computational cost but reasonable accuracy, with the idea that materials predicted with initial calculations to have especially interesting properties can be studied more carefully with detailed methods. Xu et al. introduced one approach to this challenge by using a training set of dozens of MOFs to assign charges based on the connectivity of atoms in each structure.<sup>14</sup> A strong limitation of

Received: November 17, 2011

Published: February 13, 2012

this method is that it can only be used for materials that have the same kinds of connectivities observed in the initial training set. More recently, Wilmer and Snurr used charge equilibration (Qeq) to examine 14 different MOFs.<sup>15</sup> The Qeq approach is a semiempirical technique that has been widely used since its introduction by Rappe and Goddard.<sup>16</sup> Wilmer and Snurr performed calculations for MOFs using finite clusters, so choices must be made for each material in terms of truncating the structure before calculations can be performed.

In this paper, we describe an application of the Qeq charge assignment technique that is applicable to the fully periodic structure of MOFs. We compare the results from our method, which we refer to as PQeq, with charges from the Qeq method of Wilmer and Snurr and with quantum chemistry calculations that describe electrostatic interactions with MOF frameworks in a fully rigorous way. Using calculations based on fully periodic structures rather than cluster calculations makes the examination of large numbers of materials an easier task. To demonstrate the suitability of this technique for examining large numbers of materials, we present results for CO<sub>2</sub> and N<sub>2</sub> adsorption in ~500 distinct MOFs. This is the largest set of predictions for the adsorption of these gas species in MOFs that is currently available.

Our calculations identify a number of materials that are predicted to have adsorption selectivities for CO<sub>2</sub> over N<sub>2</sub> far larger than any material identified to date. Materials that show strong selectivity for this separation have drawn considerable attention because of the critical role of this separation in postcombustion capture of CO<sub>2</sub>.<sup>1,17,18</sup> For the most promising materials identified by our initial calculations, we performed more detailed computational simulations with high quality point charges derived from quantum chemistry calculations to assess gas diffusion and mixture adsorption. These calculations are a useful illustration of the concept of coupling screening of large numbers of candidate MOFs with detailed studies of selected materials to find new materials for particular applications. More importantly, they identify two MOFs that are predicted to have extraordinary properties for adsorption-based separation of CO<sub>2</sub> and N<sub>2</sub>.

## THEORY

The Qeq method assigns point charges based on the relative location of the atoms and the atomic values for the electron affinity and ionization potential. The method was originally developed for finite clusters<sup>16</sup> and was later extended to include the effect of an infinite lattice surrounding the unit cell in the case of periodic structures.<sup>19</sup> In the Qeq formulation the energy of an atom as a function of its charge is expressed as the first two terms of a Taylor expansion series around its neutral state.

$$E_A = E_{A0} + Q_A \left( \frac{\partial E}{\partial Q} \right)_{A0} + \frac{1}{2} Q_A^2 \left( \frac{\partial^2 E}{\partial Q^2} \right)_{A0} \quad (1)$$

This can be written as

$$E_A = E_{A0} + \chi_A^0 Q_A + \frac{1}{2} J_{AA}^0 Q_A^2 \quad (2)$$

where the first and second derivatives have been defined as the electronegativity,  $\chi_A^0$ , and idempotential,  $J_{AA}^0$ , respectively. These values can be derived from atomic data.

The charge-dependent energy of a set of atoms is the summation of the energy of each atom plus the contribution of the interatomic interactions:

$$E_Q(Q_1 \dots Q_N) = \sum_A (E_{A0} + \chi_A^0 Q_A) + \frac{1}{2} \sum_{A,B} Q_A Q_B J_{AB} \quad (3)$$

Here, interatomic interactions only include charge–charge interactions. The Qeq method seeks solutions such that the first derivative of this expression in respect to the charge  $Q_A$  will be equal for all the atoms at equilibrium. The derivative, which can also be identified as a chemical potential, is

$$x_A(Q_1 \dots Q_N) = \frac{\partial E_Q}{\partial Q_A} = \chi_A^0 + J_{AA}^0 Q_A + \sum_{B \neq A} J_{AB} Q_B \quad (4)$$

Setting  $x_A$  equal for the  $N$  atoms in a system gives  $N - 1$  equations. When combined with the equation for the total charge of the system  $Q_{\text{tot}} = \sum_{i=1}^N Q_i$ , a system with  $N$  equations and  $N$  unknowns (the charges on each atom) is defined and can be solved.

In our implementation, the required atomic parameters,  $\chi_A^0$  and  $J_{AA}^0$ , were taken from the universal force field (UFF). A limited set of these parameters were reported in the original Qeq paper.<sup>16,19</sup> We obtained the parameters for the first 96 elements of the periodic table from the UFF force field implementation in the Open Babel software.<sup>20,21</sup> The values are listed in the Supporting Information.

The interatomic interaction term,  $J_{AB}$ , cannot be calculated simply as a Coulomb repulsion term because a shielding correction should be applied at close distances. This interaction is calculated as a two-center electron repulsion integral where the atomic charge densities are calculated using single spherical Slater orbitals as described in the original Qeq paper.<sup>16</sup> The calculation of the integral was carried out as described in the work by Kitao et al.<sup>22</sup> There are possible approximations for calculating this interaction term,<sup>23</sup> but they are not used in the current implementation of the method.

The extension of this method from a finite cluster of atoms to a periodic framework<sup>19</sup> requires the effect of the lattice to be incorporated in the expression for the chemical potential. This gives

$$x_{A,\text{periodic}}(Q_1 \dots Q_N) = \chi_A^0 + \chi_{c,A}^0 + J_{AA}^0 Q_A + \sum_{B \neq A} J_{AB} Q_B \quad (5)$$

where  $\chi_{c,A}^0$  is the lattice electronegativity, defined as

$$\chi_{c,A}^0 = \sum_{L \neq 0} \sum_j J'_{ij,L} + \sum_{L \neq 0} \sum_j \frac{Q_A}{R_{ij,L}} \quad (6)$$

Here, the effect of the lattice has been separated into two parts that can be calculated rigorously. The index  $L$  refers to the periodic images of the unit cell with the central unit cell denoted as  $L = 0$ .  $J'_{ij,L}$  represents the cloud penetration term (shielding correction) that is given by  $J'_{ij,L} = J_{ij,L} - 1/R$ , where the first term on the right-hand side is the interatomic interaction defined above. The cloud penetration term converges to zero rapidly with respect to the interatomic distance,  $R$ . The second summation above involving  $Q_A/R_{ij,L}$  is

a direct Coulomb interaction term which we calculate in our implementation using an Ewald summation. Applying the periodic version of Qeq to a MOF requires only the lattice parameters for a single unit cell of the material and the atomic coordinates for all atoms within the unit cell.

Because the lattice electronegativity is a nontrivial function of the individual atomic charges, the set of equations defining the charges must be solved iteratively. As in the original Qeq method, the effective charge parameter  $\zeta$  and the idempotential for hydrogen are charge dependent and are updated after each iteration.<sup>16</sup> The charges on each atom are constrained to lie within chemically meaningful boundaries. For example, Na is not allowed to take on a charge larger than +1. Below we will refer to charges assigned with this approach as PQeq charges. When the method was initially applied to assign charges to MOFs, we observed convergence issues for several structures. These were overcome, in most cases, by introducing a damping factor to average the updated values of the lattice electronegativity and hydrogen parameters with the values from the previous iterations.

## RESULTS

**Comparison with Previous Point Charge Assignments for MOFs.** Wilmer and Snurr<sup>15</sup> recently assigned point charges to 14 MOFs using a version of the Qeq method suitable for finite clusters of atoms. These calculations included a modification to the Qeq method that allowed the Taylor expansion to be centered around charged atoms or neutral atoms. This allowed the results to be in better agreement with point charges assigned using ChelpG than Qeq calculations that use a Taylor expansion centered only around neutral atoms. However, this approach requires user input regarding the expected charge on each atom type. We will refer to this method as modQeq. For comparison with the charges assigned by Wilmer and Snurr's modQeq method, we assigned charges using our implementation of PQeq on the periodic framework for the same 14 MOFs. The structure names and CSD Refcodes are shown in Table 1. All structures, except Mg/DOBDC, were obtained from the Cambridge Structural Database (CSD).<sup>24</sup>

Most of the structures were obtained from the CSD without modification, but IRMOF-1, MOF-177, Mg/DOBDC,

**Table 1. Structure Names and CSD Refcodes for the Structures Used To Compare Charges with the Work of Wilmer and Snurr<sup>15</sup>**

structure name	CSD Refcode
HKUST-1	FIQCEN
Pd(2-pymo) <sub>2</sub>	YEGCUJ
IRMOF-1	SAHYIK
Zn/DOBDC	WOBHIF
Ni/DOBDC	LECQEQ
Co/DOBDC	SATNOR
ZIF-8	OFERUN
MIL-47	IDIWIB
Zn <sub>2</sub> (NDC) <sub>2</sub> (DPNI)	MATVAF
IRMOF-3	EDUSUR
MOF-177	ERIRIG
Mg/DOBDC	–
UMCM-1	KISXIU
UMCM-150	PIVBEC

UMCM-1, and UMCM-150 required manual modifications. These modifications included removing solvent atoms and extra framework atoms present due to crystallographic disorder and adding hydrogen atoms that were not resolved in the reported crystal structures. Details of these modifications are described in the Supporting Information. To compare the assigned charges, the framework atoms were grouped in the same manner as in Wilmer and Snurr.<sup>15</sup> In cases where the charges for some of the atoms within a group were not identical due to small deviations from perfect symmetry in the crystal structures, the charges reported below are averages of the charges in the group of atoms.

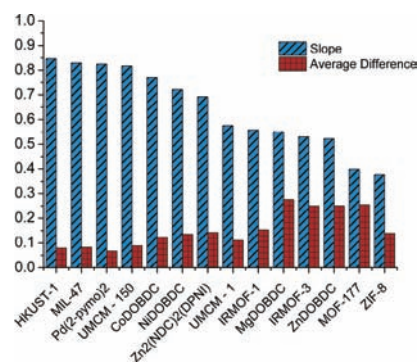


**Figure 1.** Comparison between the modQeq and PQeq method for 14 MOFs. The quantities plotted are the slope of the least-squares fit to a linear relation between the modQeq and PQeq charges and the average absolute difference between the charges value.

We compared our results with the results of Wilmer and Snurr in two ways (Figure 1): the slope of the least-squares fit to a linear equation relating the modQeq charges to the PQeq charges, and the average absolute difference between the charge values for each structure. It is clear that the PQeq charges are systematically smaller than the modQeq charges. This is expected, because our PQeq method uses values for the ionization potential and electron affinity of the neutral atoms, while the modQeq approach used charged atoms in some cases. As a result, the PQeq charges tend to be smaller in magnitude, particularly for the charges on metal atoms and the oxygen atoms bound to metals. For example, the charge on the Zn atom for IRMOF-1 is calculated to be 1.16 using modQeq and 0.46 using PQeq. The rest of the charges for IRMOF-1, however, have consistent sign and relative charge values between the two methods. For example, the difference between the charges is 0.1, 0.04, and 0.01 for the three types of C atoms and 0.03 for the H atoms. The average absolute differences between the two sets of charges for the set of 14 MOFs vary from 0.07 to 0.28.

Although the PQeq and modQeq results are not identical, the comparison above indicates that they give broadly similar results. As implemented here, the PQeq approach has the advantages that no decisions need to be made regarding termination of a molecular cluster (because the fully periodic structure is used) and no user information is required to decide which reference states should be used in the Taylor expansion. We have not implemented the use of charged-atom reference states within PQeq because, as we will show below, other more detailed charge assignment methods<sup>12</sup> can be used to make high quality charge assignments after a material of interest has been identified using PQeq-based methods.

Above, we compared approximate point charges assigned using PQeq with approximate point charges from an earlier variation of the Qeq method. A more important test of the PQeq charges comes from comparing them with the most rigorous treatments of electrostatics within MOFs that are available. To this end, we applied the PQeq approach to the recent work of Watanabe et al.,<sup>13</sup> which directly used the electrostatic potential energy surface (EPES), as calculated using DFT, to perform Grand Canonical Monte Carlo (GCMC) calculations and calculate isotherms for four MOFs. Calculations based on the DFT-EPES do not require assigning point charges to each atom in the MOF and can be viewed as a rigorous solution to the challenge of defining electrostatic interactions within a rigid, nonpolarizable MOF. For each MOF, the Henry's constant for CO<sub>2</sub> adsorption was computed from the DFT-EPES as well as from point charges derived from the Hirshfeld,<sup>28</sup> DDEC,<sup>12</sup> and REPEAT<sup>11</sup> methods. In these calculations, the CO<sub>2</sub> Lennard–Jones interactions used the same EPM2 potential<sup>25</sup> as used by Watanabe et al.;<sup>13</sup> the exact values used are shown in Table 2. For the framework–CO<sub>2</sub>

**Table 2. Force Field Parameters for Guest Molecules**

		LJ parameters		partial charges (e)
		$\epsilon/kb$ (K)	$\sigma$ (Å)	
CO <sub>2</sub> <sup>25</sup>	C	28.129	2.757	0.6512
(C–O distance: 1.149 Å)	O	80.507	3.033	–0.3256
N <sub>2</sub> <sup>26</sup>	N	36	3.31	–0.482
(N–CofM distance: 0.55 Å)	CofM	0	0	0.964
CH <sub>4</sub> <sup>27</sup>		148.2	3.812	0

interactions, we used the UFF<sup>29</sup> parameters for the framework combined with the guest parameters using the Lorentz–Berthelot mixing rules (Table 2).

The Henry's constants for CO<sub>2</sub> calculated with PQeq charges are compared to the results with the DFT-EPES in Table 3. The PQeq results show both positive and negative deviations from the correct results, with the largest deviation occurring for ZIF-90. Crucially, however, the PQeq charges allow the four materials to be correctly ranked by their CO<sub>2</sub> Henry's constants. Calculations performed without charges, however, cannot make this ranking correctly; they incorrectly predict that ZIF-90 has a Henry's constant smaller than that of ZIF-8 and give a Henry's constant for ZIF-90 that is only slightly larger than that of IRMOF-1. The corresponding results using REPEAT charges range from –10.3% to 2.0%, from –17.9% to 3.8% for DDEC charges, and from –57.1% to 2.8% for the Hirshfeld method. It is clear that the results from the PQeq charges are less accurate than GCMC calculations based on point charges assigned with DDEC or REPEAT, but charge assignment with either of these methods requires performing a DFT calculation for the fully periodic structure. As emphasized

by Watanabe et al., however, once a DFT calculation has been performed, one can use the DFT-EPES to describe electrostatics in the MOF without assigning point charges at all, at least for calculations using a rigid model of the MOF structure.<sup>13</sup> The results above represent only a small number of structures, but they indicate that the PQeq approach is capable of capturing the effect of the electrostatic interactions with reasonable accuracy with very little computational cost in a way that is applicable to any periodic structure.

**Grid-Based Calculation of Henry's Constants for CO<sub>2</sub> and N<sub>2</sub> Adsorption.** The PQeq charge assignment creates a useful basis for screening large numbers of MOFs in terms of their adsorption properties for quadrupolar or polar species. We used this idea to examine a large number of MOF materials in terms of their adsorption affinity for CO<sub>2</sub> and N<sub>2</sub>, by quantifying the Henry's constants for each adsorbate. Henry's constants can be computed using GCMC, but they can also be expressed in terms of integrals over the volume of the adsorbing material<sup>30</sup> and the degrees of freedom within the adsorbing species. In earlier work<sup>8,9</sup> we applied this formulation for adsorbates that can be represented as spheres to predict, for example, the Henry's constants for CH<sub>4</sub> and H<sub>2</sub> adsorption in thousands of silica zeolite structures.<sup>9</sup> To use this approach for CO<sub>2</sub> and N<sub>2</sub>, we extended our earlier calculations to rigid nonspherical molecules that have three translational and two rotational degrees of freedom. Integration of the adsorbate degrees of freedom was performed by applying a Monte Carlo integration scheme that randomly sampled center-of-mass locations on a grid that covered the unit cell volume. At each center-of-mass, multiple randomly chosen molecular orientations were sampled. The grid spacing used was 0.2 Å, and seven orientations were sampled at each grid point. This kind of calculation could equivalently sample the center of mass positions randomly using all locations rather than a finely spaced grid. We opted to use the grid-based approach because it took full advantage of the information that was already required for geometric characterization. The Henry's constant computed from the integration was averaged for blocks of 1000 sampled center-of-mass locations. The standard deviation of these block-averaged values was calculated every 10 000 moves, and the simulation ended when the value of the standard deviation dropped below 5% of the cumulative mean value. The number of orientations sampled was found to be sufficient to obtain adequate convergence when compared to sample calculations using larger numbers of orientations. The aim of our current calculations was to quantify the Henry's constant with acceptable precision in a fully automated manner. It can, of course, be computed to higher precision by performing more sampling. The Lennard–Jones parameters for CO<sub>2</sub>, N<sub>2</sub>, and CH<sub>4</sub> are listed in Table 2, and the interaction parameters with the framework were determined as described above for the case of CO<sub>2</sub>.

**Table 3. Comparison of the Henry's Constants for CO<sub>2</sub> Adsorption for Four MOFs at 303 K in mmol·g<sup>–1</sup>·atm<sup>–1</sup>**

	DFT-EPES <sup>α</sup>	PQeq	DDEC <sup>α</sup>	REPEAT <sup>α</sup>	no charge
IRMOF-1	0.83	0.76 (–8.4%)	0.85 (+3.0%)	0.84 (2.0%)	0.71 (–14.5%)
ZIF-8	1.75	1.46 (–16.7%)	1.44 (–17.9%)	1.65 (–6.1%)	1.36 (–22.2%)
ZIF-90	3.04	4.31 (41.8%)	2.54 (–16.3%)	2.73 (–10.3%)	0.91 (–70.1%)
Zn(nicotinate) <sub>2</sub>	109.00	117.55 (7.8%)	114 (3.8%)	107 (–1.8%)	109.5 (0.5%)

<sup>α</sup>The EPES, DDEC, and REPEAT results are from Watanabe et al.<sup>13</sup> The percentage difference from the EPES results is shown in parentheses.

**Table 4.** Comparison of the Henry's Constant Value Calculated from Fitting the Adsorption Isotherms As Determined from GCMC and from the Direct Calculation for Four MOFs (all units are in  $\text{mmol}\cdot\text{g}^{-1}\cdot\text{atm}^{-1}$ )

	from isotherm		direct calculation	
	PQeq	no charges	PQeq	no charges
IRMOF-1	0.76	0.71	0.74 (−2.5%)	0.70 (2.0%)
ZIF-8	1.46	1.36	1.47 (0.6%)	1.37 (0.3%)
ZIF-90	4.31	0.91	4.57 (6.1%)	0.95 (4.0%)
Zn(nicotinate) <sub>2</sub>	117.55	109.50	124.39 (5.8%)	112.45 (2.7%)

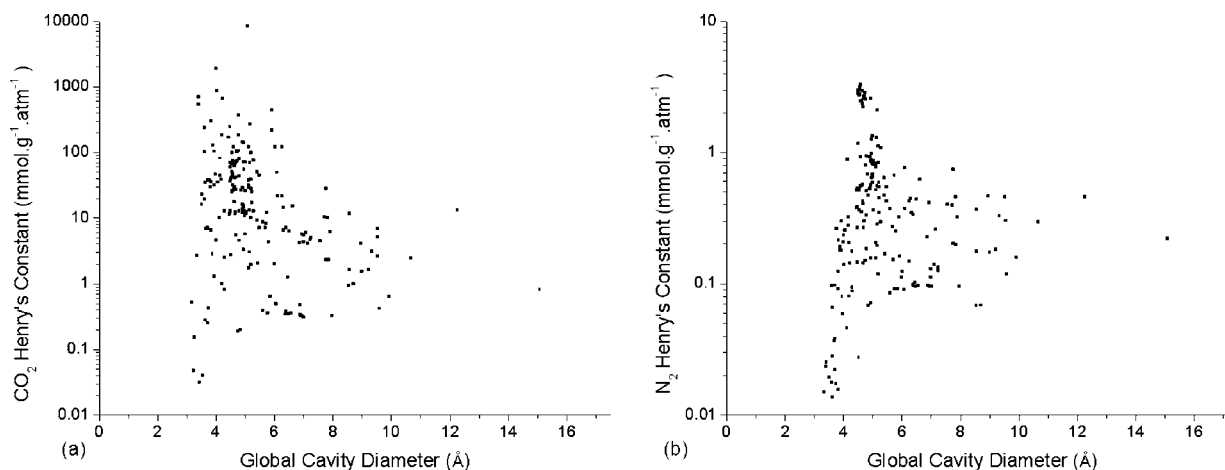
**Figure 2.** Henry's constants calculated with PQeq charges for (a)  $\text{CO}_2$  and (b)  $\text{N}_2$  at 303 K as a function of the global cavity diameter. Only the results for materials with a value larger than  $0.01 \text{ mmol}\cdot\text{g}^{-1}\cdot\text{atm}^{-1}$  are shown.

Table 4 lists the Henry's constants for four MOFs calculated with and without charges from two methods: fitting the low pressure range of the isotherm determined using GCMC, and the direct calculation. The numbers in parentheses in the table are the percentage difference between the two calculation methods. The agreement is within 6% in every case. This implies that the direct approach gives sufficient precision for screening large numbers of materials. The direct approach is better suited to this task for two reasons. First, fitting a Henry's constant to GCMC results requires the adsorbed amount to be determined at multiple pressures. Second, some preliminary GCMC calculations are typically necessary for a new material to establish the pressure range where Henry's law is valid. As a result, our direct calculations offer a numerically efficient method to compute the Henry's constants for rigid molecules in a large number of materials.

#### Screening of MOFs for Selective $\text{CO}_2/\text{N}_2$ Adsorption.

We now demonstrate an initial application of our methods to screen a large collection of MOFs and select materials with desirable properties. To this end, we consider the challenge of finding MOFs that exhibit high adsorption selectivities for  $\text{CO}_2/\text{N}_2$ . This gas separation is central to capturing  $\text{CO}_2$  from power-plant flue gases. The adsorption selectivity for  $\text{CO}_2$  over  $\text{N}_2$  is only one of multiple properties that are important in this application; any practically useful material must be robust in the presence of water and acid gas impurities, and it must be possible to synthesize the material at a large scale for reasonable cost, for example.<sup>1</sup> Nevertheless, MOFs with low  $\text{CO}_2/\text{N}_2$  selectivity cannot be competitive with other low-cost sorbents such as activated carbon in a large scale process. In our earlier work, we examined the  $\text{CH}_4/\text{H}_2$  adsorption selectivity of 500 MOFs.<sup>8</sup> Here, we examine the  $\text{CO}_2/\text{N}_2$  adsorption selectivity of the same materials using PQeq charges to describe electrostatic interactions between the molecules and the

MOFs. We successfully obtained charges for 489 materials and limited our analysis to these materials. The remaining 11 materials did not yield converged charges. The convergence issue existing in a small fraction of the materials should be addressed in future implementations of the method. For each of the analyzed structures, we calculated the Henry's constant for  $\text{CO}_2$  and  $\text{N}_2$  as described above. We also calculated the Henry's constants for  $\text{CH}_4$  in order to estimate the adsorption selectivity of  $\text{CO}_2$  over  $\text{N}_2$  and  $\text{CH}_4$ . The adsorption selectivity in the limit of low pressures is exactly equal to the ratio of Henry's constants, regardless of the composition of the gas mixture being considered.<sup>31</sup> All calculations were performed at 303 K.

In Figure 2 the calculated Henry's constants at 303 K are shown for  $\text{CO}_2$  and  $\text{N}_2$  as a function of the global cavity diameter of the MOF. The global cavity diameter is the size of the largest sphere that can fit inside the framework without overlap. This cavity is not necessarily part of the main pore channel of the framework<sup>8</sup> and might not even be accessible to the adsorbate molecules in materials with strong diffusion limitations.<sup>32</sup> This possibility can readily be dealt with when individual materials that appear attractive based on this initial characterization are examined in more detail. Only materials with a value for the Henry's constant larger than  $0.01 \text{ mmol}\cdot\text{g}^{-1}\cdot\text{atm}^{-1}$  are shown. This choice excludes 284(290) materials for  $\text{CO}_2$  ( $\text{N}_2$ ). For small pore materials, the Henry's constant for spherical adsorbates is strongly correlated with the global cavity diameter.<sup>8,9</sup> As the global cavity diameter becomes smaller than  $\sim 3 \text{ \AA}$ , the overlap between adsorbed  $\text{CO}_2$  or  $\text{N}_2$  and the framework atoms is so large that the Henry's constant drops to very small values. For cavities slightly larger than this size, however, Henry's constants spanning over 5 orders of magnitude are observed. Although the global cavity diameter is, at best, a crude descriptor of  $\text{CO}_2$  and  $\text{N}_2$  adsorption affinity, it

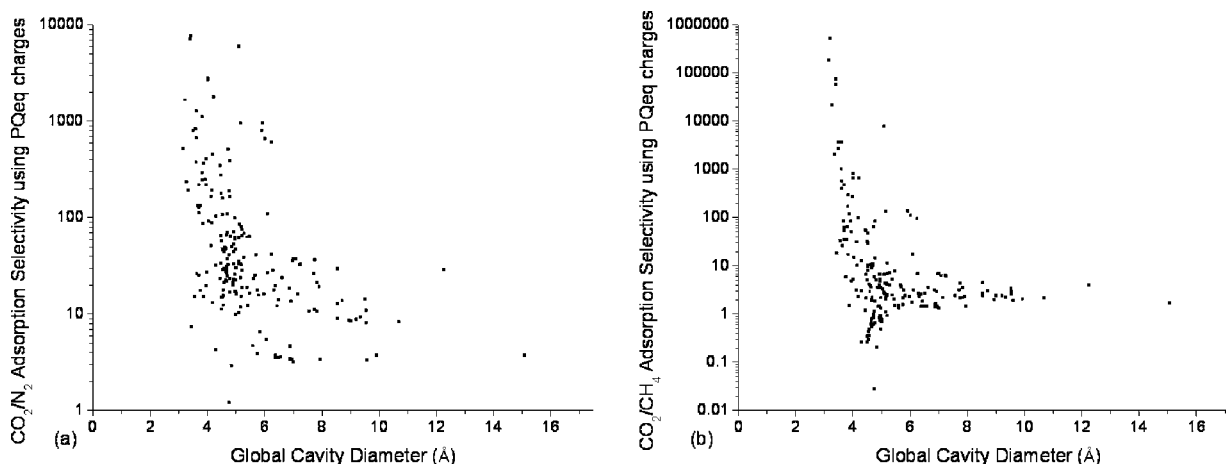


**Figure 3.** (a)  $\text{CO}_2/\text{N}_2$  and (b)  $\text{CO}_2/\text{CH}_4$  infinite dilution adsorption selectivity at 303 K for materials found to have a  $\text{CO}_2$  Henry's constant larger than  $0.01 \text{ mmol}\cdot\text{g}^{-1}\cdot\text{atm}^{-1}$ .

still gives a useful way to characterize trends among materials. Our results show that the highest Henry's constants for both  $\text{CO}_2$  and  $\text{N}_2$  are found for cavity sizes between 4 and 6 Å. For cavities of this size, the adsorbates can maximize their interactions with all the surrounding walls of the pore.

The clear difference in the magnitude of the Henry's constant for  $\text{CO}_2$  relative to  $\text{N}_2$  gives rise to considerable adsorption selectivity for many of the materials we have considered. These selectivities are shown in Figure 3a, where the  $\text{CO}_2/\text{N}_2$  selectivity as a function of the global cavity diameter is plotted for all of the materials shown in Figure 2. For all of these materials the predicted  $\text{CO}_2/\text{N}_2$  selectivity is larger than 1. We also used our previously calculated values of the Henry's constants for  $\text{CH}_4$  to define the  $\text{CO}_2/\text{CH}_4$  infinite dilution adsorption selectivity for the materials analyzed in this work.<sup>8</sup> These results are shown in Figure 3b. Unlike  $\text{CO}_2/\text{N}_2$  mixtures, it is interesting to observe that an apparent “reverse” selectivity in  $\text{CO}_2/\text{CH}_4$  mixtures is predicted for 29 materials. That is,  $\text{CH}_4$  would be preferentially adsorbed in these materials relative to  $\text{CO}_2$ . These are materials with a global cavity diameter  $\sim 4$  Å, where  $\text{CH}_4$  can adsorb very strongly. This result would only be physically interesting if these cavities are readily accessible to  $\text{CH}_4$  on experimentally relevant time scales. We used methods developed in our earlier work to analyze the diffusion properties of  $\text{CH}_4$  in each of these 29 materials.<sup>8</sup> Each material was found to have a pore limiting diameter (PLD) value less than 2.4 Å. This characterization is based on holding the MOF structure rigid, but it is a clear indication that the internal cavities in these materials are most likely inaccessible to  $\text{CH}_4$ . Using our previously described method for determining the energy barrier to diffusion,<sup>8</sup> we found that all of these materials have diffusion activation energies for  $\text{CH}_4$  larger than 114 kJ/mol, implying that the diffusion rates of  $\text{CH}_4$  in these materials are essentially zero.

Overall, 47 (52) materials were predicted to have an infinite dilution adsorption selectivity for  $\text{CO}_2/\text{N}_2$  ( $\text{CO}_2/\text{CH}_4$ ) larger than 100 (10) at 303 K. These predictions were made using the PQeq point charges in order to calculate the Henry's constants for  $\text{CO}_2$  and  $\text{N}_2$ . The PQeq charges are only an approximate treatment of the electrostatics. To address the accuracy of these predictions, we selected six structures that were predicted to have high  $\text{CO}_2/\text{N}_2$  selectivities in calculations based on PQeq charges but low selectivity in calculations that did not use any charges. For each material, we assigned point charges to the

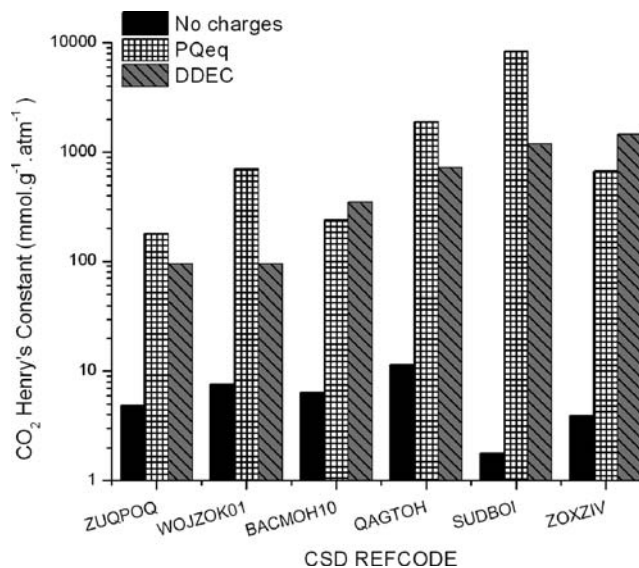


**Figure 4.** Comparison of the  $\text{CO}_2$  Henry's constant at 303 K for six MOFs without using charges (black bars), using PQeq charges (white bars), and using DDEC charges (grey bars).

MOF using DDEC charges<sup>12</sup> and recalculated the  $\text{CO}_2$  and  $\text{N}_2$  Henry's constants using these charges. The results for the  $\text{CO}_2$  Henry's constants without using charges, with PQeq charges, and with DDEC charges are shown in Figure 4. A similar plot for  $\text{N}_2$  can be found in the Supporting Information.

There are sizable quantitative differences between the results computed using PQeq and DDEC charges. For example, the  $\text{CO}_2$  Henry's constant with PQeq is 7.3 times larger (2 times smaller) for WOJZOK01 (ZOZXIV) than the results using DDEC. For the same six materials, the  $\text{CO}_2$  Henry's constants computed without point charges differ from the DDEC results by factors of 12–660. The range of Henry's constants predicted for the full set of materials above spans  $>5$  orders of magnitude. These observations indicate that results based on PQeq charges are sufficiently accurate to select the materials with the highest performance, even though it is important that more precise methods are then applied to these materials. This can also be seen from Figure 5 wherein the same comparison as in Figure 4 has been made for the  $\text{CO}_2/\text{N}_2$  and  $\text{CO}_2/\text{CH}_4$  selectivities. All of the six materials found to be highly selective using PQeq

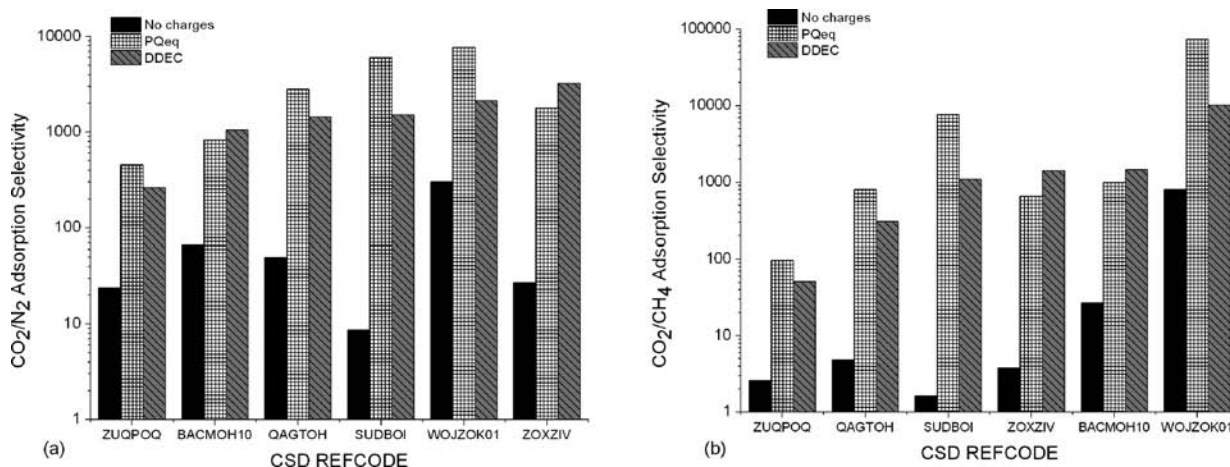


**Figure 5.** Comparison of the (a)  $\text{CO}_2/\text{N}_2$  and (b)  $\text{CO}_2/\text{CH}_4$  infinite dilution selectivity at 303 K for six MOFs without using charges (black bars), using PQeq charges (red bars), and using DDEC charges (blue bars).

charges were also found to be highly selective with the DDEC charges. These results illustrate how our screening procedure is able to process a large number of materials and correctly identify materials with exceptional properties for a specific adsorption-based separation.

An experimentally viable material must satisfy two important requirements that we have not addressed so far. First, it must have thermal and structural framework stability after the solvent molecules have been evacuated. The second requirement is that the material should allow appreciable diffusion of the targeted molecule. So far we have assumed that the examined frameworks can exist at the experimentally measured coordinates at the temperature modeled (303 K) and without the presence of any solvent atoms. The original experimental reports for the six materials listed above, however, suggest that most of them do not maintain structural stability after the removal of solvent. Specifically, of the six materials we discussed earlier, only WOJZOK01<sup>33</sup> appears to be structurally stable. Unfortunately, as will be discussed below, this material appears to be effectively nonporous for  $\text{CO}_2$  when the diffusivity of  $\text{CO}_2$  through the MOF is considered.

In order to identify experimentally viable materials that are promising for separating  $\text{CO}_2$  from  $\text{N}_2$  we examined the original experimental reports for all the materials in Figure 3 that were found to have an infinite dilution adsorption selectivity  $>100$ . From this procedure, we selected five materials that were reported to be stable after solvent removal. We then assigned DDEC charges for each of these MOFs and recalculated the  $\text{CO}_2$  and  $\text{N}_2$  Henry's constants at 303 K. The comparison for the  $\text{CO}_2/\text{N}_2$  selectivity is shown for these materials in Figure 6. Comparison of the  $\text{CO}_2$  and  $\text{N}_2$  Henry's constants, and  $\text{CO}_2/\text{CH}_4$  infinite dilution-selectivity, are shown in the Supporting Information (Figures S3–S6). Again, the general agreement is fair and the enhanced selectivity due to the effect of the electrostatic interactions is captured in all five materials. It is interesting to note that the material ECOWOI (RINPEJ) yields a  $\text{CO}_2/\text{N}_2$  selectivity using DDEC charges that is about 20 (12) times higher than by using the PQeq charges. This is an example where PQeq charges give a result that is accurate enough for initial screening purposes but where this approach gives results that differ considerably from the final result from more accurate methods. This indicates that a considerable disagreement can arise in the adsorption

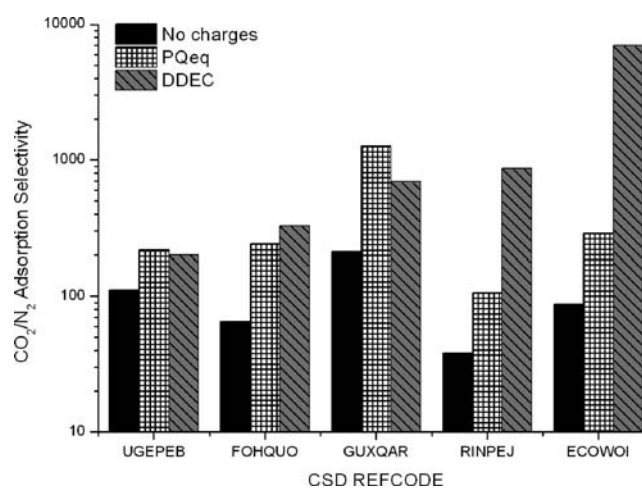


**Figure 6.** Comparison of the  $\text{CO}_2/\text{N}_2$  infinite dilution selectivity at 303 K for five selected MOFs without using charges (black bars), using PQeq charges (red bars), and using DDEC charges (blue bars).

selectivity, but the PQeq charges give a selectivity that is high enough to indicate the potential of the material for the separation. In both cases, the  $\text{CO}_2/\text{N}_2$  selectivity with the PQeq charges is about 3 times higher than without charges.

To understand whether the diffusion kinetics of molecules in these materials would be problematic toward their application in a separation process, we performed molecular dynamics (MD) calculations to calculate the diffusivity of  $\text{CO}_2$  and  $\text{N}_2$  in the materials of interest. The MD calculations were performed at the infinite dilution limit and a temperature of 303 K using methods we have described in detail previously.<sup>9,34,35</sup> For each simulation,  $1.5 \times 10^7$  canonical MC moves and  $1.5 \times 10^7$  MD steps were performed in order to equilibrate the system. Following equilibration, 20 ns trajectories were run using a time step of 1 fs, and the self-diffusivity was measured by averaging 20 independent trajectories. The results of the MD calculations for  $\text{CO}_2$  and  $\text{N}_2$  for the examined materials are shown in Table 5. As in all the calculations described in this work, these results assume that the MOFs are rigid. The MD calculations cannot give precise results for diffusion coefficients smaller than  $\sim 10^{-8} \text{ cm}^2/\text{s}$ , and therefore cases of very slow diffusion are indicated by using this value as an upper bound in Table 5.

Table 5. The Pore Limiting Diameter and CO<sub>2</sub> and N<sub>2</sub> Infinite Dilution Self-Diffusivities for 11 Selected MOFs at 303 K

CSD Refcode	PLD (Å)	self-diffusivity (cm <sup>2</sup> /s) using DDEC charges		self-diffusivity (cm <sup>2</sup> /s) using no charges	
		CO <sub>2</sub>	N <sub>2</sub>	CO <sub>2</sub>	N <sub>2</sub>
GUXQAR	2.859	<1.00 × 10 <sup>-8</sup>	<1 × 10 <sup>-8</sup>	3.15 × 10 <sup>-5</sup>	2.52 × 10 <sup>-5</sup>
ECOWOI	2.829	2.21 × 10 <sup>-7</sup>	9.10 × 10 <sup>-7</sup>	1.26 × 10 <sup>-6</sup>	5.98 × 10 <sup>-7</sup>
FOHQQUO	3.004	7.06 × 10 <sup>-6</sup>	2.56 × 10 <sup>-6</sup>	5.82 × 10 <sup>-5</sup>	6.00 × 10 <sup>-6</sup>
UGEPEB	2.904	3.05 × 10 <sup>-6</sup>	3.04 × 10 <sup>-7</sup>	9.64 × 10 <sup>-6</sup>	1.02 × 10 <sup>-6</sup>
RINPEJ	3.062	<1.00 × 10 <sup>-8</sup>	1.30 × 10 <sup>-7</sup>	2.21 × 10 <sup>-5</sup>	8.52 × 10 <sup>-7</sup>
WOJZOK01	1.409	<1.00 × 10 <sup>-8</sup>	<1.00 × 10 <sup>-8</sup>	<1.00 × 10 <sup>-8</sup>	<1.00 × 10 <sup>-8</sup>
ZOXZIV	2.908	<1.00 × 10 <sup>-8</sup>	1.49 × 10 <sup>-7</sup>	8.82 × 10 <sup>-6</sup>	1.12 × 10 <sup>-6</sup>
BACMOH10	3.079	<1.00 × 10 <sup>-8</sup>	2.75 × 10 <sup>-7</sup>	2.09 × 10 <sup>-5</sup>	4.68 × 10 <sup>-6</sup>
ZUQPOQ	3.389	2.46 × 10 <sup>-5</sup>	3.85 × 10 <sup>-5</sup>	6.32 × 10 <sup>-5</sup>	3.48 × 10 <sup>-5</sup>
SUDBOI	2.353	1.63 × 10 <sup>-6</sup>	<1 × 10 <sup>-8</sup>	6.47 × 10 <sup>-5</sup>	9.09 × 10 <sup>-5</sup>
QAGTOH	1.055	<1.00 × 10 <sup>-8</sup>	<1 × 10 <sup>-8</sup>	1.26 × 10 <sup>-8</sup>	<1.00 × 10 <sup>-8</sup>

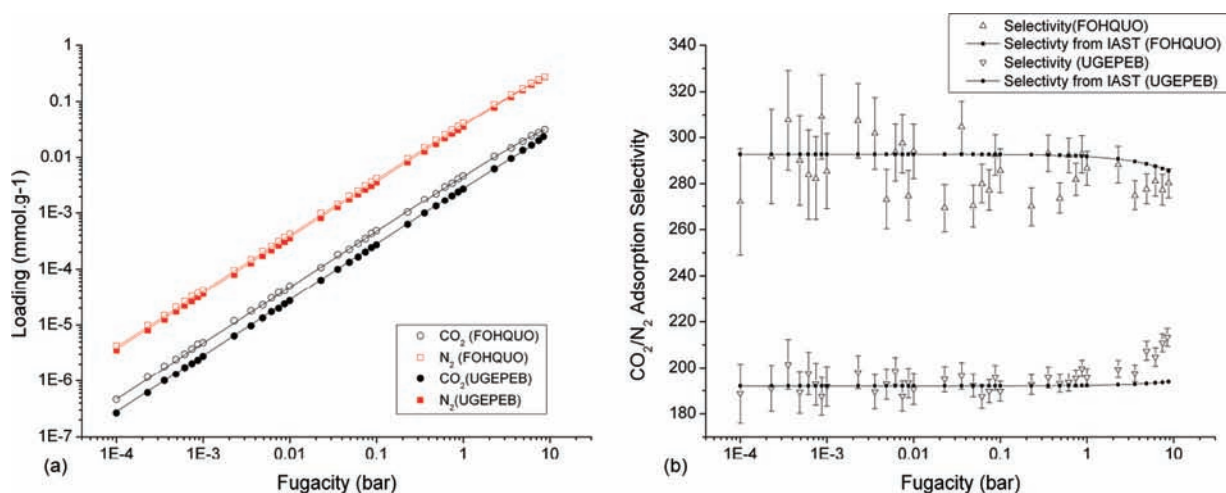


**Figure 7.** (a) Binary isotherms at a molar gas composition of 400 ppm CO<sub>2</sub> balance N<sub>2</sub> at 303 K for the MOFs FOHQQUO (empty symbols) and UGEPEB (filled symbols). The symbols are data from GCMC, and the lines are IAST predictions based on single component isotherms. The uncertainties for the GCMC data are smaller than the size of the symbol used. (b) CO<sub>2</sub>/N<sub>2</sub> selectivities for the isotherms in part a for the GCMC (empty symbols) and IAST (filled symbols).

For at least five materials, the calculated diffusivity of N<sub>2</sub> is larger than CO<sub>2</sub>. This is a clear indication that it is not simply the kinetic diameter of these molecules that controls diffusion in these MOFs but that the influence of electrostatics on diffusion is also important. In order to validate this observation, we calculated the diffusivities for each MOF without including electrostatic interactions. These results are also shown in Table 5. For all five materials, the N<sub>2</sub>-selective diffusion effect is lost when no charges are used. In many of the materials, the inclusion of charges causes large changes in the calculated diffusivities. These observations confirm that the electrostatic charge distributions in these materials play a decisive role in the diffusion of N<sub>2</sub> and CO<sub>2</sub>.

From the 11 materials examined in detail, two MOFs (UGEPEB and FOHQQUO), that satisfy both the requirement for stability and for fast CO<sub>2</sub> diffusion, stand out. UGEPEB has the chemical formula (C<sub>6</sub>H<sub>5</sub>CuNO<sub>3</sub>)<sub>n</sub>·n(H<sub>2</sub>O). The structural stability of the framework is retained up to 225 °C after the guest water molecules are removed.<sup>36</sup> The framework has one-dimensional pores along the *a*-axis with a pore limiting diameter of 2.90 Å. The CO<sub>2</sub> self-diffusivity was calculated to be 1.0 × 10<sup>-5</sup> cm<sup>2</sup>/s at infinite dilution and 303 K. Our calculations predicted that N<sub>2</sub> diffusion in this material was roughly 1 order of magnitude slower, but this diffusion is still rapid enough to allow equilibration of N<sub>2</sub> inside the pores on

experimentally relevant time scales. Our calculations using DDEC charges for this MOF predict a CO<sub>2</sub>/N<sub>2</sub> adsorption selectivity of 328 at 303 K in Henry's law regime. FOHQQUO has the chemical formula (C<sub>6</sub>H<sub>14</sub>CoO<sub>13</sub>Sr)<sub>n</sub>·2n(H<sub>2</sub>O). On the basis of TGA measurements,<sup>37</sup> guest water loss occurs from 70 °C to 190 °C and the framework remains stable until about 350 °C. Like UGEPEB, FOHQQUO has one-dimensional pores, in this case with a pore limiting diameter of 3.00 Å. The CO<sub>2</sub> self-diffusivity, calculated at the same conditions as that for UGEPEB, was 2.70 × 10<sup>-6</sup> cm<sup>2</sup>/s, and the N<sub>2</sub> diffusivity was approximately 1 order of magnitude smaller. The predicted CO<sub>2</sub>/N<sub>2</sub> adsorption selectivity at infinite dilution and 303 K for this material was 200.

So far we have limited all of our calculations to Henry's law regime, which enables us to perform a large number of calculations, because adsorbate–adsorbate interactions are neglected. However, it is important to examine the materials under realistic conditions that involve higher pressures and mixtures of adsorbates that are relevant for applications. To address this issue, we used GCMC to calculate binary isotherms for CO<sub>2</sub>/N<sub>2</sub> mixtures. We considered two molar compositions of CO<sub>2</sub>/N<sub>2</sub> gas mixtures which are of interest for large-scale applications. First, we considered a mixture with 400 ppm CO<sub>2</sub> and the balance N<sub>2</sub>, which corresponds to dry air. Then we considered a mixture with 15% CO<sub>2</sub> and 85% N<sub>2</sub>, which is

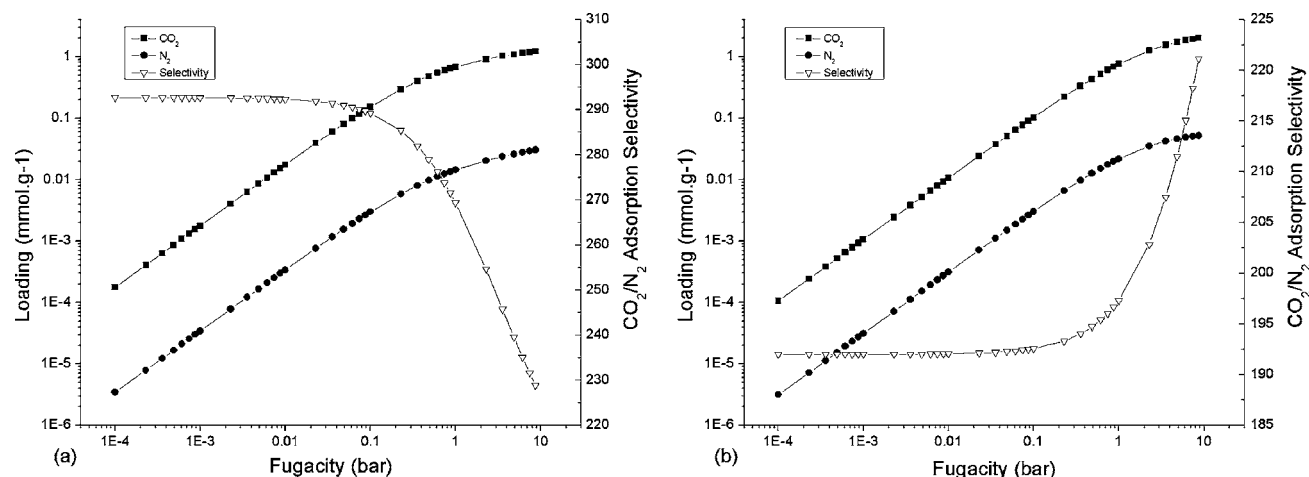


**Figure 8.**  $\text{CO}_2/\text{N}_2$  binary isotherm and corresponding selectivity at 303 K calculated using IAST for the MOFs (a) FOHQQU and (b) UGEPEB, at a molar gas composition of 15%  $\text{CO}_2/85\%$   $\text{N}_2$ .

representative of dry flue gas from coal-fired power plants. It is difficult to obtain well equilibrated GCMC results when the adsorbed phase is much richer in one of the species. This situation is precisely what is expected in a highly selective adsorbent in equilibrium with a gas mixture containing moderate amounts of multiple species. One way to overcome this limitation is to obtain single-component isotherms and then apply ideal adsorbed solution theory (IAST)<sup>38</sup> to predict the binary isotherm. IAST often gives accurate results for nanoporous materials such as MOFs, except in the case of energetic heterogeneity between the adsorbates.<sup>39,40</sup>

In Figure 7, we validate the accuracy of IAST for each material using conditions where we can perform accurate binary GCMC calculations. We used GCMC to calculate the binary isotherm for 400 ppm  $\text{CO}_2$  balance  $\text{N}_2$  (dry air) for all 11 selective materials listed above. These calculations used DDEC charges for the electrostatic interactions and the same Lennard–Jones parameters as for the Henry’s constant calculations. Each isotherm was calculated at 303 K for a fugacity range of  $10^{-4}$  to 10 bar. As with the previous calculations, the framework atoms were kept rigid at their crystallographic positions. The binary isotherms for FOHQQU and UGEPEB are shown in Figure 7a. The binary isotherms for the other nine materials are in the Supporting Information. Also shown in Figure 7a are the predicted binary isotherms using IAST (solid lines). The IAST results were obtained by fitting the single component isotherms with a Langmuir isotherm constrained to have the correct Henry’s constant. It is seen that IAST gives very accurate predictions for FOHQQU and UGEPEB.

The adsorption selectivity for a binary mixture is given by the ratio of the gas compositions of the adsorbed phase relative to the ratio of the gas compositions in the gas phase. Figure 7b shows the calculated binary selectivities for FOHQQU and UGEPEB. The selectivities show little variation within the fugacity range examined and have an average of 286 for FOHQQU and 195 for UGEPEB. The other nine materials were all found to be highly selective based on the binary isotherms (Supporting Information). These observations validate the use of the Henry’s constant as a screening criterion for identifying promising materials. The high selectivities of these materials mean that accurate GCMC calculations are not feasible for 15%  $\text{CO}_2/85\%$   $\text{N}_2$  gas mixtures. The results above,

however, indicate that IAST will give accurate results for these conditions. IAST results for this gas mixture are shown in Figure 8 for FOHQQU and for UGEPEB. At low total pressures, the selectivities are the same as for the 400 ppm  $\text{CO}_2$  gas mixture, but as the fugacity increases and the isotherms begin to saturate, the selectivity decreases for FOHQQU and increases for UGEPEB. For a 15%  $\text{CO}_2/85\%$   $\text{N}_2$  mixture at 1 (10) atm and 303 K, the predicted selectivity is 269 (227) for FOHQQU. For UGEPEB, the selectivity at the same conditions is predicted to be 197 (223). Besides high selectivity, a high  $\text{CO}_2$  capacity is also a desirable property for a material to be interesting for a carbon capture application. FOHQQU has a  $\text{CO}_2$  capacity at 0.1 (1) bar of 11.8 (52.9) mg/g, and for UGEPEB the capacity is 3.7 (27.0) mg/g. These values are comparable to the capacity of MOF-177 at 1 bar (35 mg/g)<sup>41</sup> and the capacities of the materials considered by Wilmer et al.,<sup>15</sup> which range from 3.5 to 80 mg/g at 0.1 bar. Therefore, the two materials identified here are highly selective while maintaining a considerable  $\text{CO}_2$  capacity.

Our calculations have identified two MOFs that appear to have very promising properties for highly selective adsorption of  $\text{CO}_2$  from  $\text{N}_2$ . Both materials have been experimentally reported to be stable upon solvent removal, and our MD calculations indicate that adsorbed  $\text{CO}_2$  and  $\text{N}_2$  are not subject to strong diffusion limitations. The adsorption selectivity predicted for these materials appears to be very high relative to other similar materials that have been reported previously. Our calculations involve some important limitations. In particular, they only examined dry gases, so we cannot comment on the stability or selectivity of these materials in the presence of water vapor, which is ubiquitous in practical applications. Nevertheless, we feel that our results make these two materials excellent candidates for experimental evaluation.

## CONCLUSIONS

We have performed a large-scale computational screening of MOF materials, focusing on the identification of promising materials for adsorption-based separations. We have expanded upon our previous efforts with spherical adsorbates<sup>8,9</sup> and are now able to reliably account for electrostatic interactions during large-scale screening and also screen the materials for interactions with nonspherical adsorbates. Our results show that these methods are applicable to large numbers of

structures, which is a requirement of any attempt to systematically examine the large number of existing MOFs. In order to account for electrostatic interactions on a large scale, we implemented a periodic charge equilibration method (PQeq),<sup>19</sup> which can be directly applied to the periodic structure of MOFs. Although we observed considerable differences between the charges assigned by the present methods and those assigned by previous methods, the PQeq charges were found to describe the electrostatic interactions adequately for materials screening purposes.

We used the Henry's constant of adsorption as the key quantity of interest for initial screening of materials for adsorption-based separations. We were able to calculate the Henry's constant for a large collection of materials using a direct numerical integration over the potential energy surface of the adsorbed phase. Materials found to have a high selectivity in the infinite dilution limit using PQeq charges can be examined in more detail at finite loading using well established GCMC and MD methods. Additionally, more precise methods to describe the electrostatic interactions can be used. We applied this approach to ~500 MOFs by assigning PQeq charges to them and calculating their Henry's constants at 303 K for CO<sub>2</sub> and N<sub>2</sub>. Together with our previously calculated results for CH<sub>4</sub>,<sup>8</sup> we were able to compute CO<sub>2</sub>/N<sub>2</sub> and CO<sub>2</sub>/CH<sub>4</sub> selectivities. We then chose 11 highly selective materials, assigned DDEC<sup>12</sup> point charges to them, and recalculated more accurate Henry's constants for CO<sub>2</sub> and N<sub>2</sub>. All the materials were also found to be highly selective using DDEC charges.

Not all of the 11 shortlisted materials are experimentally viable candidates because of their lack of structural stability and undesirable transport properties. After systematically excluding the materials that are known to lack structural stability or exhibit very slow CO<sub>2</sub> diffusion (in MD calculations), we focused on the two remaining materials. We further examined these materials by calculating binary isotherms at 303 K for dry air and flue gas compositions by GCMC and IAST methods, respectively. The materials were found to be highly selective (selectivities >190) over all the conditions examined, making them promising candidate materials for CO<sub>2</sub> capture applications. To determine the viability of these materials in realistic applications, it would of course also be necessary to understand their performance in the presence of humid gases and gas-phase contaminants such as SO<sub>x</sub> and NO<sub>x</sub>. In our view, these important issues are best addressed experimentally. Because we only examined a fraction of the MOFs that have been reported in the literature, we are confident that many more interesting materials remain to be discovered for a range of applications. The approaches we have presented here are applicable to thousands of materials and can be further extended for large-scale screening and identification of materials for the diffusion properties of nonspherical, polar molecules.

## ■ ASSOCIATED CONTENT

### 📄 Supporting Information

Isotherms and other information about the MOFs simulated in this work. This material is available free of charge via the Internet at <http://pubs.acs.org>.

## ■ AUTHOR INFORMATION

### Corresponding Author

[david.sholl@chbe.gatech.edu](mailto:david.sholl@chbe.gatech.edu)

## Notes

The authors declare no competing financial interest.

## ■ ACKNOWLEDGMENTS

This work was supported by ConocoPhillips Company. The authors acknowledge Dr. K. C. McCarley and Dr. J. Drese (ConocoPhillips) for useful discussions.

## ■ REFERENCES

- (1) Keskin, S.; Van Heest, T. M.; Sholl, D. S. *ChemSusChem* **2010**, *3*, 879.
- (2) Han, S. S.; Mendoza-Cortes, J. L.; Goddard, W. A. *Chem. Soc. Rev.* **2009**, *38*, 1460.
- (3) Kuppler, R. J.; Timmons, D. J.; Fang, Q.-R.; Li, J.-R.; Makal, T. A.; Young, M. D.; Yuan, D.; Zhao, D.; Zhuang, W.; Zhou, H.-C. *Coord. Chem. Rev.* **2009**, *253*, 3042.
- (4) Li, J.-R.; Kuppler, R. J.; Zhou, H.-C. *Chem. Soc. Rev.* **2009**, *38*, 1477.
- (5) Meek, S. T.; Greathouse, J. A.; Allendorf, M. D. *Adv. Mater.* **2011**, *23*, 249.
- (6) Keskin, S.; Liu, J.; Rankin, R. B.; Johnson, J. K.; Sholl, D. S. *Ind. Eng. Chem. Res.* **2008**, *48*, 2355.
- (7) Duren, T.; Bae, Y.-S.; Snurr, R. Q. *Chem. Soc. Rev.* **2009**, *38*, 1237.
- (8) Haldoupis, E.; Nair, S.; Sholl, D. S. *J. Am. Chem. Soc.* **2010**, *132*, 7528.
- (9) Haldoupis, E.; Nair, S.; Sholl, D. S. *Physical Chem. Chem. Phys.* **2011**, *13*, 5053.
- (10) Wilmer, C. E.; Leaf, M.; Lee, C. Y.; Farha, O. K.; Hauser, B. G.; Hupp, J. T.; Snurr, R. Q. *Nat. Chem.* **2012**, *4*, 83–89.
- (11) Campaña, C.; Mussard, B.; Woo, T. K. *J. Chem. Theory Comput.* **2009**, *5*, 2866.
- (12) Manz, T. A.; Sholl, D. S. *J. Chem. Theory Comput.* **2010**, *6*, 2455.
- (13) Watanabe, T.; Manz, T. A.; Sholl, D. S. *J. Phys. Chem. C* **2011**, *115*, 4824.
- (14) Xu, Q.; Zhong, C. *J. Phys. Chem. C* **2010**, *114*, 5035.
- (15) Wilmer, C. E.; Snurr, R. Q. *Chem. Eng. J.* **2011**, *171*, 775.
- (16) Rappe, A. K.; Goddard, W. A. *J. Phys. Chem.* **1991**, *95*, 3358.
- (17) Yazaydin, A. O.; Snurr, R. Q.; Park, T.-H.; Koh, K.; Liu, J.; LeVan, M. D.; Benin, A. I.; Jakubczak, P.; Lanuza, M.; Galloway, D. B.; Low, J. J.; Willis, R. R. *J. Am. Chem. Soc.* **2009**, *131*, 18198.
- (18) Britt, D.; Furukawa, H.; Wang, B.; Glover, T. G.; Yaghi, O. M. *Proc. Natl. Acad. Sci. U.S.A.* **2009**, *106*, 20637.
- (19) Ramachandran, S.; Lenz, T. G.; Skiff, W. M.; Rappe, A. K. *J. Phys. Chem.* **1996**, *100*, 5898.
- (20) Guha, R.; Howard, M. T.; Hutchison, G. R.; Murray-Rust, P.; Rzepa, H.; Steinbeck, C.; Wegner, J.; Willighagen, E. L. *J. Chem. Inf. Model.* **2006**, *46*, 991.
- (21) The Open Babel Package, version 2.2.3 <http://openbabel.sourceforge.net/>, 2011.
- (22) Kitao, O.; Ogawa, T. *Mol. Phys.* **2003**, *101*, 3.
- (23) Louwen, J. N.; Vogt, E. T. C. *J. Mol. Catal. A: Chem.* **1998**, *134*, 63.
- (24) Allen, F. *Acta Crystallogr. Sect. B* **2002**, *58*, 380.
- (25) Harris, J. G.; Yung, K. H. *J. Phys. Chem.* **1995**, *99*, 12021.
- (26) Potoff, J. J.; Siepmann, J. I. *AIChE J.* **2001**, *47*, 1676.
- (27) Jiang, S. Y.; Gubbins, K. E.; Zollweg, J. A. *Mol. Phys.* **1993**, *80*, 103.
- (28) Hirshfeld, F. L. *Theor. Chem. Acc.* **1977**, *44*, 129.
- (29) Rappe, A. K.; Casewit, C. J.; Colwell, K. S.; Goddard, W. A.; Skiff, W. M. *J. Am. Chem. Soc.* **1992**, *114*, 10024.
- (30) June, R. L.; Bell, A. T.; Theodorou, D. N. *J. Phys. Chem.* **1990**, *94*, 1508.
- (31) Challa, S. R.; Sholl, D. S.; Johnson, J. K. *J. Chem. Phys.* **2002**, *116*, 814.
- (32) Krishna, R.; van Baten, J. M. *Langmuir* **2009**, *26*, 2975.
- (33) Lin, W.; Ma, L.; Evans, O. R. *Chem. Commun.* **2000**, 2263.
- (34) Skoulidas, A. I.; Sholl, D. S. *J. Phys. Chem. B* **2002**, *106*, 5058.
- (35) Sholl, D. S. *Acc. Chem. Res.* **2006**, *39*, 403.

- (36) Lin, C. Z. J.; Chui, S. S. Y.; Lo, S. M. F.; Shek, F. L. Y.; Wu, M.; Suwinska, K.; Lipkowski, J.; Williams, I. D. *Chem. Commun.* **2002**, 1642.
- (37) Gil de Muro, I.; Insausti, M.; Lezama, L.; Pizarro, J. L.; Arriortua, M. I.; Rojo, T. *Eur. J. Inorg. Chem.* **1999**, 1999, 935.
- (38) Myers, A. L.; Prausnitz, J. M. *AIChE J.* **1965**, *11*, 121.
- (39) Murthi, M.; Snurr, R. Q. *Langmuir* **2004**, *20*, 2489.
- (40) Chen, H.; Sholl, D. S. *Langmuir* **2007**, *23*, 6431.
- (41) Millward, A. R.; Yaghi, O. M. *J. Am. Chem. Soc.* **2005**, *127*, 17998.